ELSEVIER

Journal of Alloys and Compounds 404–406 (2005) 533–536

Journal of ALLOYS AND COMPOUNDS

www.elsevier.com/locate/jallcom

Mechanically driven b.c.c. TiCr alloy and its hydrogen solubility

H. Yabe[a], T. Kuji[b,*]

[a] *Japan Society for the Promotion Science, Japan*
[b] *Course of Materials Science and Technology, Graduate School of High-Technology for Human Welfare, Tokai University, 317 Nishino, Numazu, Shizuoka 410-0395, Japan*

Received 6 September 2004; received in revised form 26 January 2005; accepted 31 January 2005
Available online 14 July 2005

Abstract

In this study, Ti–Cr binary mixtures were prepared by mechanical alloying and the phase structure and corresponding hydrogen solubility were discussed. According to the binary equilibrium phase diagram, solubility of Ti in Cr at room temperature is very limited. This is because Ti is in equilibrium with the extremely stable Laves phase ($TiCr_2$) existing in the middle of the phase diagram. In this study, it was demonstrated that mechanically alloying yielded formation of Ti–Cr b.c.c. phase at room temperature. It was discussed how the excess energy derived during mechanical alloying works on the formation of Ti–Cr b.c.c. phase. *P–C* isotherms of the synthesized Ti–Cr alloy powders show the capability of hydrogen absorption and desorption. Especially, the $Ti_{80}Cr_{20}$ hydride should be very stable so that the high hydrogen content around 2 wt.% even at 10^{-4} MPa was shown. In addition, the $Ti_{80}Cr_{20}$ hydride was identified as f.c.c. structure with hydrogen content was 3.4 wt.% at 5.5 MPa and 313 K.

Keywords: Mechanical alloying; Titanium–chromium; Crystal structure; b.c.c.; Hydrogen solubility

1. Introduction

Hydrogen storage alloys have attracted growing interest as one of the most important materials for ecology, i.e., hydrogen storage for fuel cells and hydrogen vehicles, and human friendly soft actuator for rehabilitation [1]. The most important property to be considered for practical hydrogen storage materials is the capacity of hydrogen near room temperature.

The hydrogen absorbing properties of body center cubic (b.c.c.) solid solution alloys have shown many attractive results in the literature [2–7]. It is well known that the large hydrogen solubility in b.c.c. alloys is created by the structure transformations accompanied with the hydrogen absorption from b.c.c. into b.c.t. and f.c.c. at higher hydrogen pressure.

Ti is one of the most attractive constitution elements for hydrogen storage alloy. It can absorb the large amount of hydrogen and it is relatively lightweight. Ti–Cr alloy is also one of the most promising hydrogen storage alloys. From the binary phase diagram, Ti has h.c.p. structure at low temperatures, $T < 1155$ K but b.c.c. structure is stable at higher temperatures, $T > 1155$ K. Cr shows a b.c.c. structure up to the melting point, $T_m = 2136$ K. The mixture of b.c.c. Ti and Cr forms solid solution over the entire composition range.

$TiCr_2$ phase is well known to be in Laves structure at low temperatures but with increasing temperature the allotropic transformation in Laves structure occurs from cubic C15 ($MgCu_2$) through hexagonal C14 ($MgZn_2$) to dehexagonal C36 ($MgNi_2$). At temperature higher than 1643 K, $TiCr_2$ is stable in b.c.c. structure in the narrow temperature range just below the conjugate high melting temperature so that it is difficult to obtain metastable b.c.c. phase by the rapid quenching techniques. However, it is known that the substituting third element is effective to lower the transformation temperature from b.c.c. to Laves structure. As the result, Ti–Cr–V and Ti–Cr–Mo ternary b.c.c. alloys were obtained by rapid quenching and their extremely high hydrogen absorption capacity, H > 3 wt.%, has been reported [3–7].

Recently, synthesis of metastable phases by mechanical alloying (MA) and mechanical grinding (MG) has been extensively studied [2,8–12]. As mentioned above, $TiCr_2$ alloy

* Corresponding author. Tel.: +81 55 968 1211x1414; fax: +81 55 968 1224.
E-mail address: tkuji@urchin.fc.u-tokai.ac.jp (T. Kuji).

0925-8388/$ – see front matter © 2005 Elsevier B.V. All rights reserved.
doi:10.1016/j.jallcom.2005.01.116

is stable to be in Laves structure at relatively lower temperatures, but it has been demonstrated that MG of $TiCr_2$ Laves phase powder yielded the formation of nanocrystalline b.c.c. solid solution [11,13]. This should imply that the energy created by repeated hard plastic deformation of powders during MG is much higher than expected. It should be mentioned here that the mechanical milling is more effective to obtain larger super-cooling state compared with the rapid solidification techniques.

In this study, the fundamental information on binary Ti–Cr b.c.c. alloys prepared by mechanical alloying will be provided. It will be discussed how the excess energy derived during mechanical alloying works on the formation of TiCr b.c.c. phase. And the corresponding hydrogen absorption properties will be discussed.

2. Experimental procedure

Elemental powders of Ti (purities 99.9%, <150 μm), and Cr (99.9%, <150 μm) were blended to reach nominal compositions of: (a) $Ti_{20}Cr_{80}$, (b) $Ti_{33}Cr_{67}$ (as $TiCr_2$), (c) $Ti_{40}Cr_{60}$, (d) $Ti_{50}Cr_{50}$, (e) $Ti_{60}Cr_{40}$ and (f) $Ti_{80}Cr_{20}$. After pre-mixing the elemental powders to the desired composition, the powder mixture was poured into a stainless steel (SUS304) container together with 1/2 in. diameter stainless steel (SUS304) balls and sealed under an argon atmosphere in a globe box. In this study, the mechanical alloying of the samples was carried out by using high-power mechanical alloying apparatus (NEV-MA8, Nissin–Giken, Japan) under argon atmosphere at room temperature for milling duration of 90 h. This apparatus allowed us to proceed mechanical alloying under continuous water-cooling because the container does not rotate. A ball-to-powder weight ratio was 40:1 with 3 g material milled at once.

Subsequently, the ethanol was poured into the container to prevent oxidation [14]. After drying, structure and hydrogen absorption/desorption properties of alloys were analyzed by the following equipments.

The phases in the mechanically alloyed powders were identified by X-ray diffraction (XRD) using Cu Kα radiation at room temperature. The thermal behavior of the MA powders was determined by a differential scanning calorimeter (DSC) at a heating rate of 20 K/min in an argon flow atmosphere. The DSC measurements were carried out in argon filled globe box. We used powder sample of 20 mg for DSC measurements. After DSC measurements, the phases in the annealed powders were also determined by XRD at room temperature. Anti-reflection silicone was used for the sample holder for annealed powders. The powder samples after MA for 90 h were put into the reaction tube and evacuated for 12 h at 673 K. After degassing treatment at 673 K, the reaction tube was rapidly cooled to RT. The pressure–composition (*P–C*) isotherms for absorption and desorption were determined using a Sievert's apparatus at 313 K up to hydrogen pressure of 10 MPa.

3. Results and discussions

3.1. Structures of synthesized Ti–Cr alloys

Fig. 1 shows the powder XRD profiles of synthesized Ti–Cr alloys with different Ti compositions. The diffraction peaks of mechanically alloyed Ti–Cr powders were highly broadened. The grain sizes, *D* calculated from the XRD peak width using Scherrer's equation were approximately 7.2 nm. It can be seen that mechanical alloying of Ti–Cr mixtures yielded the formation of single nano-sized solid solutions.

The typical XRD patterns from b.c.c. structure were obtained for powders with Ti content ≤40 at.%. The diffraction peak angles moved to lower angle with increasing Ti composition, suggesting that b.c.c. lattice was expanded by substituting Ti with larger atomic size. On the other hand, the additional peaks appeared for powders with Ti content ≥40 at.%. From the calculation of lattice parameter as shown in Fig. 2, these additional peaks were also identified to be from b.c.c. structure. In this study, the former and latter b.c.c. phases were defined as Cr-richer and Ti-richer b.c.c.'s, respectively. It is reasonable that Ti richer b.c.c. has a larger lattice constant than that of Cr richer b.c.c. so that $Ti_{50}Cr_{50}$ alloy should contain two different b.c.c. phases. It should be noticed that the lattice constant value of Ti-richer b.c.c. for $Ti_{50}Cr_{50}$, described as white square, is somewhat crude, because this value was calculated by only one XRD peak and the peaks from both phases overlap each other. In this figure, reference lattice parameter values of b.c.c. β-Ti at 1173 K and b.c.c. Cr were plotted.

The lattice parameters of Cr-richer b.c.c. alloys increased with increasing Ti content in the relatively low Ti content region. This is simply due to the dissolution of larger Ti atoms into smaller Cr lattice. Furthermore, it must be emphasized here that the excess energy derived during the mechanical alloying yields the formation of metastable

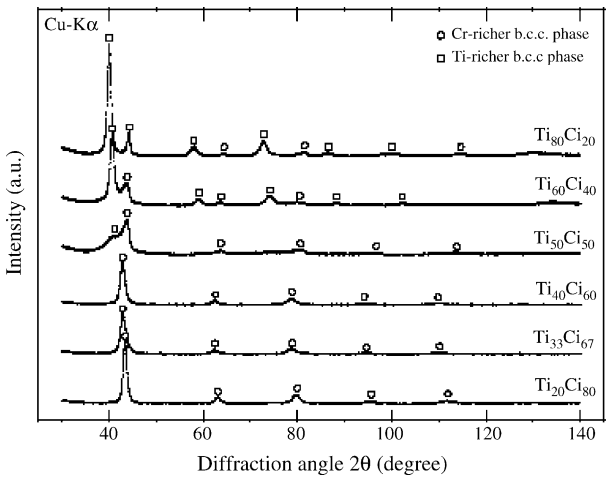

Fig. 1. XRD profiles of synthesized Ti–Cr alloys with different Ti compositions.

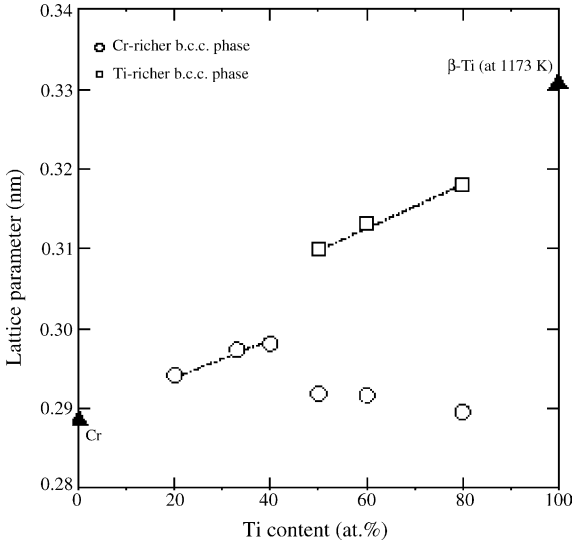

Fig. 2. Lattice parameters *a* calculated from the XRD profiles of synthesized Ti–Cr alloys.

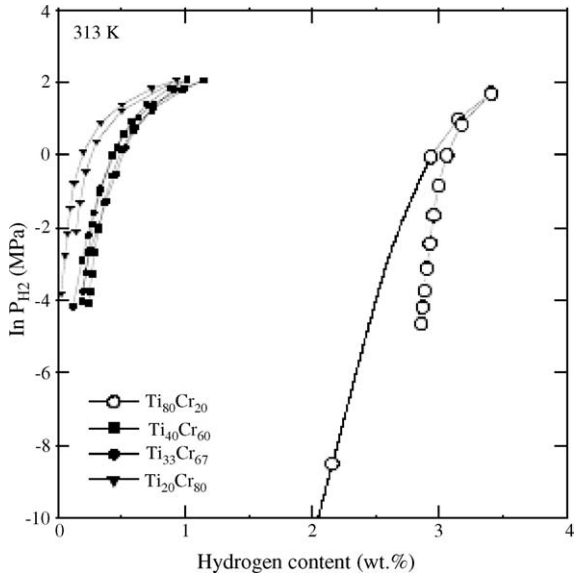

Fig. 3. Pressure–composition isotherms at 313 K for synthesized Ti–Cr alloys.

Ti–Cr b.c.c. phase at room temperature, which should appear at higher temperature according to equilibrium phase diagram.

Figs. 1 and 2 also show the diffraction patterns from the Ti side of compositions. It can be seen that above mentioned two different b.c.c. phases, i.e., Ti-richer b.c.c. and Cr-richer b.c.c, dominate the XRD patterns over the diffraction angle. These XRD patterns of Ti-richer side, typically $Ti_{50}Cr_{50}$ alloy, strongly indicate the progressing towards single-phase formation. It is, therefore, believed that excessive mechanical alloying yields a formation of single Ti-richer phase. In fact, longer time mechanical alloying for 300 h are under schedule.

In the early stages of MA, the grain size of Ti and Cr decreased with proceeding MA process. This is due to the accumulation of excess energy served to elemental powders by the hard plastic deformation. And then, when the grain size reached nano order, the mutual diffusion of each element starts occurring.

From the consideration of XRD patterns shown in Fig. 1, it seems to predict that the allotropic transformation of h.c.p. α-Ti to b.c.c. β-Ti occurred before or after initial mutual diffusion starts, suggesting that the enthalpy stored in grain boundaries could serve as a driving force for alloy formation and allotropic transformation. In this study, b.c.c. β-Ti phase appeared in the early stage of MA. Equivalent behavior was seen for Fe–Pd nano-mixtures [12].

3.2. Hydrogen absorption properties of synthesized Ti–Cr alloys

The DSC measurements were carried out from RT to 673 K. The results of the XRD diffraction patterns from heated Ti–Cr powders to 673 K show no significant change in the diffraction pattern from b.c.c. Therefore, in this study, the initial activation before hydrogenation was carried out at 673 K.

Pressure–composition isotherms at 313 K for synthesized Ti–Cr alloys are shown in Fig. 3. As mentioned previously, the hydrogen absorption of b.c.c. alloys are accompanied with structure transformations, b.c.c. → b.c.t → f.c.c. In this study, plateau pressure corresponding to the hydride formation does not clearly appear for our alloys. Plateau pressures corresponding to b.c.c. → b.c.t, for $Ti_{20}Cr_{80}$, $Ti_{33}Cr_{67}$ and $Ti_{40}Cr_{60}$ powders seem to be higher than 10 MPa. On the other hand, the $Ti_{80}Cr_{20}$ hydride should be very stable so that the high hydrogen content even at 10^{-4} MPa is around 2 wt.%. In fact, the $Ti_{80}Cr_{20}$ hydride was identified as f.c.c structure (see Fig. 4). In this study, we calculated the maximum hydrogen capacity for the hypothetical case that only Ti in Ti–Cr powder mixture absorbs hydrogen. Calculated value

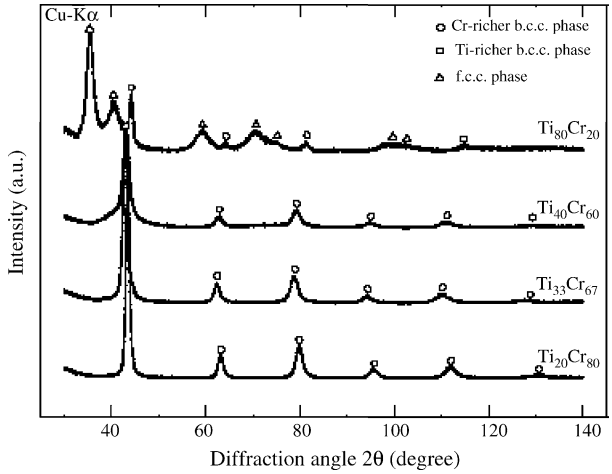

Fig. 4. XRD profiles of synthesized Ti–Cr alloys after *P–C–T* measurements.

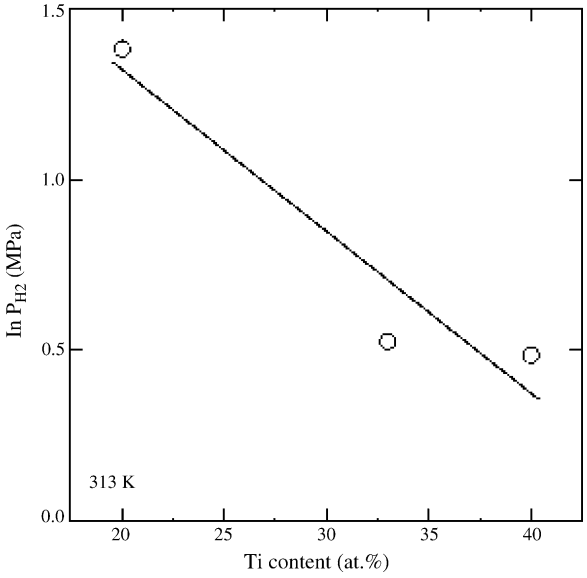

Fig. 5. Chemical potential of hydrogen for $Ti_{20-40}Cr_{8O-60}$ b.c.c. alloys at 313 K.

was 3.2 wt.%, which is in good agreement with hydrogen content in $Ti_{80}Cr_{20}$ alloys, 3.4 wt.% at 5.5 MPa and 313 K.

Generally, the stability of a metal hydride is dependent on lattice parameter and the affinity of substitute elements to hydrogen. The larger lattice should contain larger interstitial cages, expecting lower insertion energy for interstitial hydrogen atoms, leading stabilization of hydride. This is reasonable way to understand the hydride stability. In the case of Ti–Cr system, Ti element is larger than Cr so that increase in Ti content should increase lattice parameter, implying lowering plateau pressure. Moreover, the affinity of hydrogen to Ti should be much higher than Cr.

From both physical and chemical viewpoints, hydrogen absorption properties of Ti–Cr b.c.c. alloys is controlled by Ti content. Fig. 5 shows the chemical potential of hydrogen in $Ti_{20-40}Cr_{80-60}$ b.c.c. alloys at 313 K. As expected, Ti stabilizes hydride of the alloys.

Fig. 4 also shows that XRD profiles of mechanically alloyed $Ti_{80}Cr_{20}$ powders after *P–C–T* measurements. It can be seen that $Ti_{80}Cr_{20}$ alloy was fully charged by hydrogen, suggesting that the Ti-richer b.c.c. phase was transformed from b.c.c. through b.c.t. to f.c.c. In the case that the Ti content was lower than 40 at.%, the plateau pressures for absorption should be always higher than 10 MPa. Diffraction patterns from these alloys after *P–C–T* measurements, therefore, describe b.c.c. phase.

4. Conclusion

In this study, mechanical alloying yields the formation of metastable Ti–Cr b.c.c. phase at room temperature, which should appear at higher temperature according to equilibrium phase diagram. This is due to the accumulation of excess energy served to elemental powders by the hard plastic deformation. As results, two kind of b.c.c. phases with different lattice parameters were formed, i.e., Cr-richer and Ti-richer b.c.c.'s. These synthesized phases were found to be stable till 673 K.

As results of pressure–composition isotherms at 313 K, plateau pressures corresponding to b.c.c. → b.c.t, for $Ti_{20}Cr_{80}$, $Ti_{33}Cr_{67}$ and $Ti_{40}Cr_{60}$ powders seem to be higher than 10 MPa. On the other hand, the $Ti_{80}Cr_{20}$ hydride should be very stable so that the high hydrogen content even at 10^{-4} MPa is around 2 wt.%. In fact, the $Ti_{80}Cr_{20}$ hydride was identified as f.c.c. structure. The chemical potential of hydrogen in $Ti_{20-40}Cr_{80-60}$ b.c.c. alloys at 313 K also described consistently that Ti stabilizes hydride of the synthesized Ti–Cr alloys.

Acknowledgements

T.K. and H.Y. would like to acknowledge for the financial support from New Energy and Industrial Technology Development Organization (NEDO) and Tanaka precious metals Foundation. T.K. also would like to thank Tokyo Ohka Foundation for the Promotion of Science and Technology. H.Y. would like to acknowledge for the grant in the Japan Society for the Promotion of Science (JSPS).

References

[1] Y. Wakisaka, M. Muro, T. Kabutomori, H. Takeda, S. Shimizu, S. Ino, T. Ifukube, IEEE Trans. Rehab. Eng. 5 (1997) 148.
[2] T. Kuji, S. Nakayama, N. Hanzawa, Y. Tabira, J. Alloys Compd. 356–357 (2003) 456.
[3] S. Cho, C. Han, C. Park, E. Akiba, J. Alloys Compd. 288 (1999) 294.
[4] H. Arashima, F. Takahashi, T. Ebisawa, H. Itoh, T. Kabutomori, J. Alloys Compd. 356–357 (2003) 405.
[5] A. Kamegawa, T. Tamura, H. Takamura, M. Okada, J. Alloys Compd. 356–357 (2003) 447.
[6] K. Kubo, H. Itoh, T. Takahashi, T. Ebisawa, T. Kabutomori, Y. Nakamura, E. Akiba, J. Alloys Compd. 356–357 (2003) 452.
[7] T. Tamura, T. Kazumi, A. Kamegawa, H. Takamura, M. Okada, J. Alloys Compd. 356–357 (2003) 505.
[8] S. Orimo, H. Fujii, J. Alloys Compd. 232 (1996) L16.
[9] T. Aizawa, T. Kuji, H. Nakano, J. Alloys Compd. 291 (1999) 248.
[10] T. Kuji, H. Nakano, T. Aizawa, J. Alloys Compd. 330–336 (2002) 590.
[11] N. Takeichi, H. Takeshita, T. Oishi, T. Kaneko, H. Tanaka, T. Kiyobayashi, N. Kuriyama, Mater. Trans. JIM 43 (2002) 2161.
[12] H. Yabe, T. Kuji, J. Metastable Nanocryst. Mater., 2005 in press.
[13] H. Yabe, S. Nakayama, T. Kuji, Private communication (2003).
[14] H. Nakano, T. Kuji, S. Nakayama, J. Jpn. Soc., Powder Powder Metall. 41 (2004) 32.